

¹ Memory for television episodes preserves event content
² while introducing new across-event similarities

³ Andrew C. Heusser^{1,2}, Paxton C. Fitzpatrick¹, and Jeremy R. Manning^{1,*}

¹Department of Psychological and Brain Sciences

Dartmouth College, Hanover, NH 03755, USA

²Akili Interactive

Boston, MA 02110

*Corresponding author: jeremy.r.manning@dartmouth.edu

⁴ February 2, 2020

⁵ **Abstract**

The ways our experiences unfold over time define unique *trajectories* through the relevant representational spaces. Within this geometric framework, one can compare the shape of the trajectory formed by an experience to that defined by our later remembering of that experience. We propose a framework for mapping naturalistic experiences onto geometric spaces that characterize how experiences are segmented into discrete events, and how the contents of event sequences evolve over time. We apply this approach to a naturalistic memory experiment which had participants view and recount a television episode. The content of participants' recounts of events from the original episode closely matched the original episode's content. However, the similarity patterns *across* events was much different in the original episode as compared with participants' recounts. We also identified a network of brain structures that are sensitive to the "shapes" of ongoing experiences, and an overlapping network that is sensitive (at the time of encoding) to how people later remembered those experiences in relation to other experiences.

18 In this way, modeling the content of richly structured experiences can reveal how (geometrically
19 and conceptually) those experiences are segmented into events and integrated into our memories
20 of other experiences.

21 **Introduction**

22 What does it mean to *remember* something? In traditional episodic memory experiments (e.g.,
23 list-learning or trial-based experiments; Murdock, 1962; Kahana, 1996), remembering is often cast
24 as a discrete and binary operation: each studied item may be separated from all others, and la-
beled as having been recalled or forgotten. More nuanced studies might incorporate self-reported
25 confidence measures as a proxy for memory strength, or ask participants to discriminate between
26 “recollecting” the (contextual) details of an experience or having a general feeling of “familiarity”
27 (Yonelinas, 2002). Using well-controlled, trial-based experimental designs, the field has amassed
28 a wealth of valuable information regarding human episodic memory. However, there are funda-
29 mental properties of the external world and our memories that trial-based experiments are not well
30 suited to capture (for review also see Koriat and Goldsmith, 1994; Huk et al., 2018). First, our expe-
31 riences and memories are continuous, rather than discrete—removing a (naturalistic) event from
32 the context in which it occurs can substantially change its meaning. Second, the specific language
33 used to describe an experience has little bearing on whether the experience should be considered to
34 have been “remembered.” Asking whether the rememberer has precisely reproduced a specific set
35 of words to describe a given experience is nearly orthogonal to whether they were actually able to
36 remember it. In classic (e.g., list-learning) memory studies, by contrast, the number or proportion
37 of precise recalls is often a primary metric for assessing the quality of participants’ memories.
38 Third, one might remember the *essence* (or a general summary) of an experience but forget (or
39 neglect to recount) particular details. Capturing the essence of what happened is typically the
40 main “point” of recounting a memory to a listener, while the addition of highly specific details
41 may add comparatively little to successful conveyance of an experience.
42

43 How might one go about formally characterizing the “essence” of an experience, or whether

44 it has been recovered by the rememberer? Any given moment of an experience derives meaning
45 from surrounding moments, as well as from longer-range temporal associations (Lerner et al.,
46 2011; Manning, 2019). Therefore, the timecourse describing how an event unfolds is fundamental
47 to its overall meaning. Further, this hierarchy formed by our subjective experiences at different
48 timescales defines a *context* for each new moment (e.g., Howard and Kahana, 2002; Howard et al.,
49 2014), and plays an important role in how we interpret that moment and remember it later (for
50 review see Manning et al., 2015). Our memory systems can leverage these associations to form
51 predictions that help guide our behaviors (Ranganath and Ritchey, 2012). For example, as we
52 navigate the world, the features of our subjective experiences tend to change gradually (e.g., the
53 room or situation we are in at any given moment is strongly temporally autocorrelated), allowing
54 us to form stable estimates of our current situation and behave accordingly (Zacks et al., 2007;
55 Zwaan and Radvansky, 1998).

56 Although our experiences most often change gradually, they also occasionally change sud-
57 denly (e.g., when we walk through a doorway; Radvansky and Zacks, 2017). Prior research
58 suggests that these sharp transitions (termed *event boundaries*) during an experience help to dis-
59 cretize our experiences (and their mental representations) into *events* (Radvansky and Zacks, 2017;
60 Brunec et al., 2018; Heusser et al., 2018a; Clewett and Davachi, 2017; Ezzyat and Davachi, 2011;
61 DuBrow and Davachi, 2013). The interplay between the stable (within event) and transient (across
62 event) temporal dynamics of an experience also provides a potential framework for transforming
63 experiences into memories that distill those experiences down to their essence. For example, prior
64 work has shown that event boundaries can influence how we learn sequences of items (Heusser
65 et al., 2018a; DuBrow and Davachi, 2013), navigate (Brunec et al., 2018), and remember and un-
66 derstand narratives (Zwaan and Radvansky, 1998; Ezzyat and Davachi, 2011). Prior research has
67 implicated the hippocampus and the medial prefrontal cortex as playing a critical role in trans-
68 forming experiences into structured and consolidated memories (Tompry and Davachi, 2017).

69 Here we sought to examine how the temporal dynamics of a “naturalistic” experience were
70 later reflected in participants’ memories. We analyzed an open dataset that comprised behavioral
71 and functional Magnetic Resonance Imaging (fMRI) data collected as participants viewed and then

72 verbally recounted an episode of the BBC television series *Sherlock* (Chen et al., 2017). We developed
73 a computational framework for characterizing the temporal dynamics of the moment-by-moment
74 content of the episode and of participants' verbal recalls. Specifically, we use topic modeling (Blei
75 et al., 2003) to characterize the thematic conceptual (semantic) content present in each moment of
76 the episode and recalls, and Hidden Markov Models (Rabiner, 1989; Baldassano et al., 2017) to
77 discretize this evolving semantic content into events. In this way, we cast naturalistic experiences
78 (and recalls of those experiences) as *trajectories* that describe how the experiences evolve over
79 time. Under this framework, successful remembering entails verbally "traversing" the content
80 trajectory of the episode, thereby reproducing the shape (or essence) of the original experience.
81 Comparing the shapes of the topic trajectories of the episode and of participants' retellings of the
82 episode then reveals which aspects of the episode were preserved (or lost) in the translation into
83 memory. We further examine whether 1) the *precision* with which a participant recounts each event
84 and 2) the *distinctiveness* each recall event is (relative to the other recalled events) relates to their
85 overall memory performance. Last, we identify networks of brain structures whose responses
86 (as participants watched the episode) reflected the temporal dynamics of the episode, and how
87 participants would later recount the episode.

88 Results

89 To characterize the shape of the *Sherlock* episode and participants' subsequent recounts of its
90 unfolding, we used a topic model (Blei et al., 2003) to discover the latent themes in the episode's
91 dynamic content. Topic models take as inputs a vocabulary of words to consider and a collection
92 of text documents, and return two output matrices. The first of these is a *topics matrix* whose rows
93 are topics (latent themes) and whose columns correspond to words in the vocabulary. The entries
94 of the topics matrix define how each word in the vocabulary is weighted by each discovered topic.
95 For example, a detective-themed topic might weight heavily on words like "crime," and "search."
96 The second output is a *topic proportions matrix*, with one row per document and one column per
97 topic. The topic proportions matrix describes what mixture of discovered topics is reflected in each

98 document.

99 Chen et al. (2017) collected hand-annotated information about each of 1000 (manually identified)
100 scenes spanning the roughly 50 minute video used in their experiment. This information included:
101 a brief narrative description of what was happening; whether the scene took place indoors or
102 outdoors; the names of any characters on the screen; the names of any characters who were in
103 focus in the camera shot; the names of characters who were speaking; the location where the scene
104 took place; the camera angle (close up, medium, long, etc.); whether or not background music was
105 present; and other similar details (for a full list of annotated features see *Methods*). We took from
106 these annotations the union of all unique words (excluding stop words, such as “and,” “or,” “but,”
107 etc.) across all features and scenes as the “vocabulary” for the topic model. We then concatenated
108 the sets of words across all features contained in overlapping, 50-scene sliding windows, and
109 treated each 50-scene sequence as a single “document” for the purpose of fitting the topic model.
110 Next, we fit a topic model with (up to) $K = 100$ topics to this collection of documents. We found that
111 32 unique topics (with non-zero weights) were sufficient to describe the time-varying content of the
112 video (see *Methods*; Figs. 1, S2). Note that our approach is similar in some respects to Dynamic Topic
113 Models (Blei and Lafferty, 2006) in that we sought to characterize how the thematic content of the
114 episode evolved over time. However, whereas Dynamic Topic Models are designed to characterize
115 how the properties of *collections* of documents change over time, our sliding window approach
116 allows us to examine the topic dynamics within a single document (or video). Specifically, our
117 approach yielded (via the topic proportions matrix) a single *topic vector* for each timepoint of the
118 episode (we set timepoints to match the acquisition times of the 1976 fMRI volumes collected as
119 participants viewed the episode).

120 The topics we found were heavily character-focused (e.g., the top-weighted word in each topic
121 was nearly always a character) and could be roughly divided into themes that were primarily
122 Sherlock Holmes-focused (Sherlock is the titular character), primarily John Watson-focused (John
123 is Sherlock’s close confidant and assistant), or focused on Sherlock and John interacting (Fig. S2).
124 Several of the topics were highly similar, which we hypothesized might allow us to distinguish
125 between subtle narrative differences (if the distinctions between those overlapping topics were

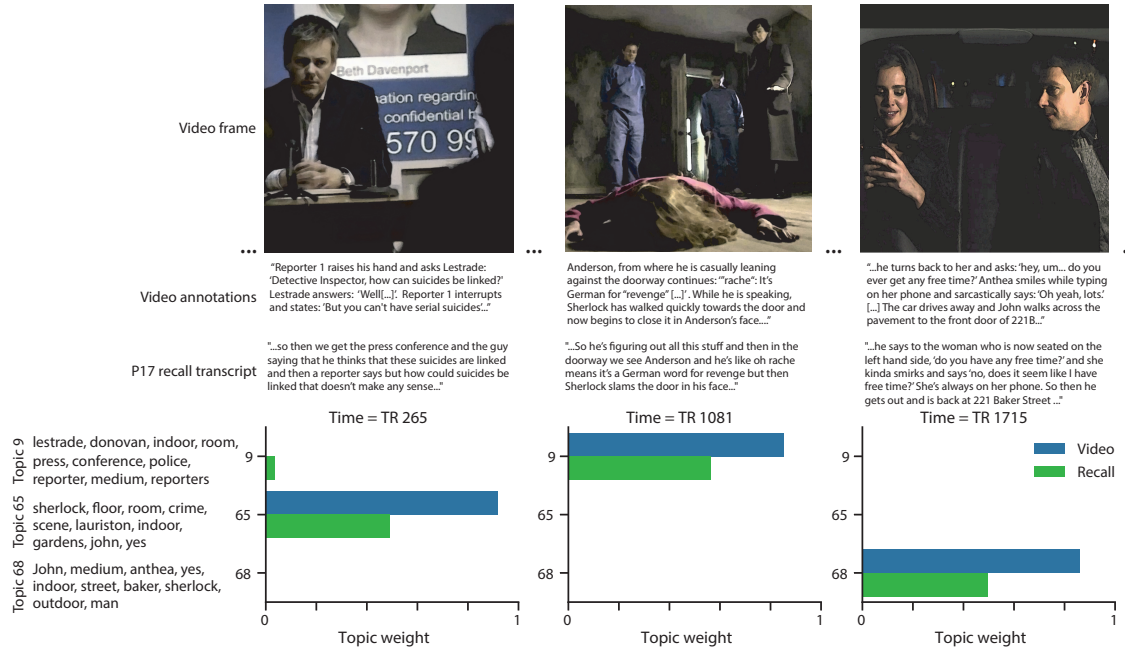


Figure 1: Methods overview. We used hand-annotated descriptions of each moment of video to fit a topic model. Three example video frames and their associated descriptions are displayed (top two rows). Participants later recalled the video (in the third row, we show example recalls of the same three scenes from participant 13). We used the topic model (fit to the annotations) to estimate topic vectors for each moment of video and each sentence the participants recalled. Example topic vectors are displayed in the bottom row (blue: video annotations; green: example participant’s recalls). Three topic dimensions are shown (the highest-weighted topics for each of the three example scenes, respectively). We also show the ten highest-weighted words for each topic. Figure S2 provides a full list of the top 10 words from each of the discovered topics.

126 meaningful; also see Fig. S3). The topic vectors for each timepoint were *sparse*, in that only a small
127 number (usually one or two) of topics tended to be “active” in any given timepoint (Fig. 2A).
128 Further, the dynamics of the topic activations appeared to exhibit *persistance* (i.e., given that a
129 topic was active in one timepoint, it was likely to be active in the following timepoint) along with
130 *occasional rapid changes* (i.e., occasionally topics would appear to spring into or out of existence).
131 These two properties of the topic dynamics may be seen in the block diagonal structure of the
132 timepoint-by-timepoint correlation matrix (Fig. 2B) and reflect the gradual drift and sudden shifts
133 fundamental to the contextual dynamics of real-world experiences. Given this observation, we
134 adapted an approach devised by Baldassano et al. (2017), and used a Hidden Markov Model (HMM)
135 to identify the *event boundaries* where the topic activations changed rapidly (i.e., at the boundaries
136 of the blocks in the correlation matrix; event boundaries identified by the HMM are outlined in
137 yellow). Part of our model fitting procedure required selecting an appropriate number of “events”
138 to segment the timeseries into. We used an optimization procedure to identify the number of
139 events that maximized within-event stability while also minimizing across-event correlations (see
140 *Methods* for additional details). To create a stable “summary” of the video, we computed the
141 average topic vector within each event (Fig. 2C).

142 Given that the time-varying content of the video could be segmented cleanly into discrete
143 events, we wondered whether participants’ recalls of the video also displayed a similar structure.
144 We applied the same topic model (already trained on the video annotations) to each participant’s
145 recalls. Analogous to how we analyzed the time-varying content of the video, to obtain similar
146 estimates for participants’ recalls, we treated each (overlapping) 10-sentence “window” of their
147 transcript as a “document” and then computed the most probable mix of topics reflected in each
148 timepoint’s sentences. This yielded, for each participant, a number-of-windows by number-of-
149 topics topic proportions matrix that characterized how the topics identified in the original video
150 were reflected in the participant’s recalls. Note that an important feature of our approach is
151 that it allows us to compare participant’s recalls to events from the original video, despite that
152 different participants may have used different language to describe the same event, and that those
153 descriptions may not match the original annotations. This is a substantial benefit of projecting



Figure 2: Modelling naturalistic stimuli and recalls. All panels: darker colors indicate greater values; range: [0, 1]. **A.** Topic vectors ($K = 100$) for each of the 1976 video timepoints. **B.** Timepoint-by-timepoint correlation matrix of the topic vectors displayed in Panel A. Event boundaries detected by the HMM are denoted in yellow (30 events detected). **C.** Average topic vectors for each of the 30 video events. **D.** Topic vectors for each of 265 sliding windows of sentences spoken by an example participant while recalling the video. **E.** Timepoint-by-timepoint correlation matrix of the topic vectors displayed in Panel D. Event boundaries detected by the HMM are denoted in yellow (22 events detected). **F.** Average topic vectors for each of the 22 recalled events from the example participant. **G.** Correlations between the topic vectors for every pair of video events (Panel C) and recalled events (from the example participant; Panel F). For similar plots for all participants see Figure S5. **H.** Average correlations between each pair of video events and recalled events (across all 17 participants). To create the figure, each recalled event was assigned to the video event with the most correlated topic vector (yellow boxes in panels G and H). The heat maps in each panel were created using Seaborn (Waskom et al., 2016).

¹⁵⁴ the video and recalls into a shared “topic” space. An example topic proportions matrix from one
¹⁵⁵ participant’s recalls is shown in Figure 2D.

¹⁵⁶ Although the example participant’s recall topic proportions matrix has some visual similarity to
¹⁵⁷ the video topic proportions matrix, the time-varying topic proportions for the example participant’s
¹⁵⁸ recalls are not as sparse as for the video (e.g., compare Figs. 2A and D). Similarly, although there
¹⁵⁹ do appear to be periods of stability in the recall topic dynamics (e.g., most topics are active or
¹⁶⁰ inactive over contiguous blocks of time), the overall timecourses are not as cleanly delineated as
¹⁶¹ the video topics are. To examine these patterns in detail, we computed the timepoint-by-timepoint
¹⁶² correlation matrix for the example participant’s recall topic proportions (Fig. 2E). As in the video
¹⁶³ correlation matrix (Fig. 2B), the example participant’s recall correlation matrix has a strong block
¹⁶⁴ diagonal structure, indicating that their recalls are discretized into separated events. As for the
¹⁶⁵ video correlation matrix, we can use an HMM, along with the aforementioned number-of-events
¹⁶⁶ optimization procedure (also see *Methods*) to determine how many events are reflected in the
¹⁶⁷ participant’s recalls and where specifically the event boundaries fall (outlined in yellow). We
¹⁶⁸ carried out a similar analysis on all 17 participants’ recall topic proportions matrices (Fig. S4).

¹⁶⁹ Two clear patterns emerged from this set of analyses. First, although every individual partic-
¹⁷⁰ ipant’s recalls could be segmented into discrete events (i.e., every individual participant’s recall
¹⁷¹ correlation matrix exhibited clear block diagonal structure; Fig. S4), each participant appeared to
¹⁷² have a unique *recall resolution*, reflected in the sizes of those blocks. For example, some participants’
¹⁷³ recall topic proportions segmented into just a few events (e.g., Participants P4, P5, and P7), while
¹⁷⁴ others’ recalls segmented into many shorter duration events (e.g., Participants P12, P13, and P17).
¹⁷⁵ This suggests that different participants may be recalling the video with different levels of detail-
¹⁷⁶ e.g., some might touch on just the major plot points, whereas others might attempt to recall every
¹⁷⁷ minor scene or action. The second clear pattern present in every individual participant’s recall
¹⁷⁸ correlation matrix is that, unlike in the video correlation matrix, there are substantial off-diagonal
¹⁷⁹ correlations. Whereas each event in the original video was (largely) separable from the others
¹⁸⁰ (Fig. 2B), in transforming those separable events into memory, participants appear to be integrat-
¹⁸¹ ing across multiple events, blending elements of previously recalled and not-yet-recalled events

182 into each newly recalled event (Figs. 2D, S4; also see Manning et al., 2011; Howard et al., 2012).

183 The above results indicate that both the structure of the original video and participants' recalls
184 of the video exhibit event boundaries that can be identified automatically by characterizing the
185 dynamic content using a shared topic model and segmenting the content into events using HMMs.
186 Next, we asked whether some correspondence might be made between the specific content of the
187 events the participants experienced in the video, and the events they later recalled. One approach
188 to linking the experienced (video) and recalled events is to label each recalled event as matching
189 the video event with the most similar (i.e., most highly correlated) topic vector (Figs. 2G, S5). This
190 yields a sequence of "presented" events from the original video, and a (potentially differently
191 ordered) sequence of "recalled" events for each participant. Analogous to classic list-learning
192 studies, we can then examine participants' recall sequences by asking which events they tended
193 to recall first (probability of first recall; Fig. 3A; Welch and Burnett, 1924; Postman and Phillips,
194 1965; Atkinson and Shiffrin, 1968); how participants most often transition between recalls of the
195 events as a function of the temporal distance between them (lag-conditional response probability;
196 Fig. 3B; Kahana, 1996); and which events they were likely to remember overall (serial position
197 recall analyses; Fig. 3C; Murdock, 1962). Interestingly, for two of these analyses (probability of first
198 recall and lag-conditional response probability curves) we observe patterns comparable to classic
199 effects from the list-learning literature: namely, a higher probability of initiating recall with the
200 first event in the sequence (Fig. 3A) and a higher probability of transitioning to neighboring events
201 with an asymmetric forward bias (Fig. 3C). In contrast, we do not observe a pattern comparable to
202 the serial position effect (Fig. 3C), but rather we see higher memory for specific events distributed
203 somewhat evenly throughout the video.

204 We can also apply two list-learning-native analyses that describe how participants group items
205 in their recall sequences: temporal clustering and semantic clustering (Polyn et al., 2009, see
206 *Methods* for details). Temporal clustering refers to the extent to which participants group their
207 recall responses according to encoding position. Overall, we found that sequentially viewed video
208 events were clustered heavily in participants' recall event sequences (mean: 0.767, SEM: 0.029),
209 and that participants with higher temporal clustering scores tended to perform better according

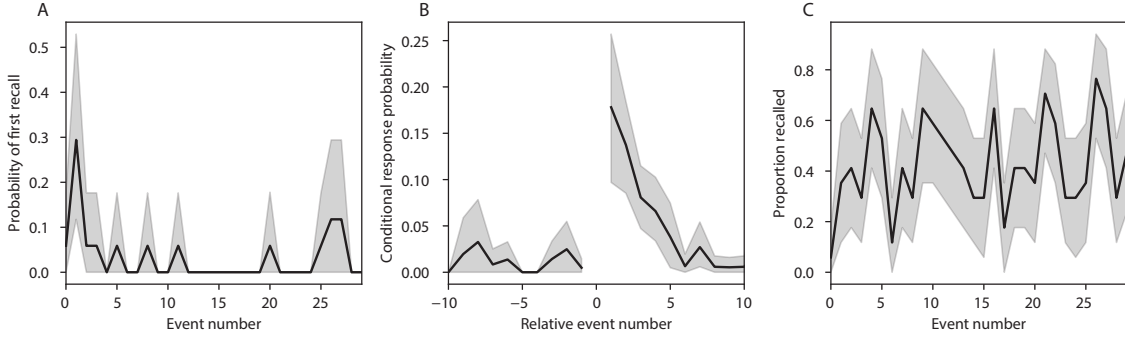


Figure 3: Naturalistic extensions of classic list-learning memory analyses. A. The probability of first recall as a function of the serial position of the event in the video. B. The probability of recalling each event, conditioned on having most recently recalled the event *lag* events away in the video. C. The proportion of participants who recalled each event, as a function of the serial position of the events in the video. All panels: error bars denote bootstrap-estimated standard error of the mean.

to both Chen et al. (2017)'s hand-annotated memory scores (Pearson's $r(15) = 0.62$, $p = 0.008$) and our model's estimate (Pearson's $r(15) = 0.54$, $p = 0.024$). Semantic clustering measures the extent to which participants cluster their recall responses according to semantic similarity. We found that participants tended to recall semantically similar video events together (mean: 0.787, SEM: 0.018), and that semantic clustering score was also related to both hand-annotated (Pearson's $r(15) = 0.65$, $p = 0.004$) and model-derived (Pearson's $r(15) = 0.63$, $p = 0.007$) memory performance.

Statistical models of memory studies often treat memory recalls as binary (e.g. the item was recalled or not) and independent events. However, our framework produces a content-based model of individual stimulus and recall events, allowing for direct quantitative comparison between all stimulus and recall events, as well as between the recall events themselves. Leveraging these content-based models of the stimulus/recall events, we developed two novel metrics for quantifying naturalistic memory representations: *precision* and *distinctiveness*. We define precision as the average correlation between the topic proportions of each recall event and the maximally correlated video event (Fig. 4). Participants whose recall events are more veridical descriptions of what happened in the video event will presumably have higher precision scores. We find that, across participants, a higher precision score is correlated to both hand-annotated memory performance

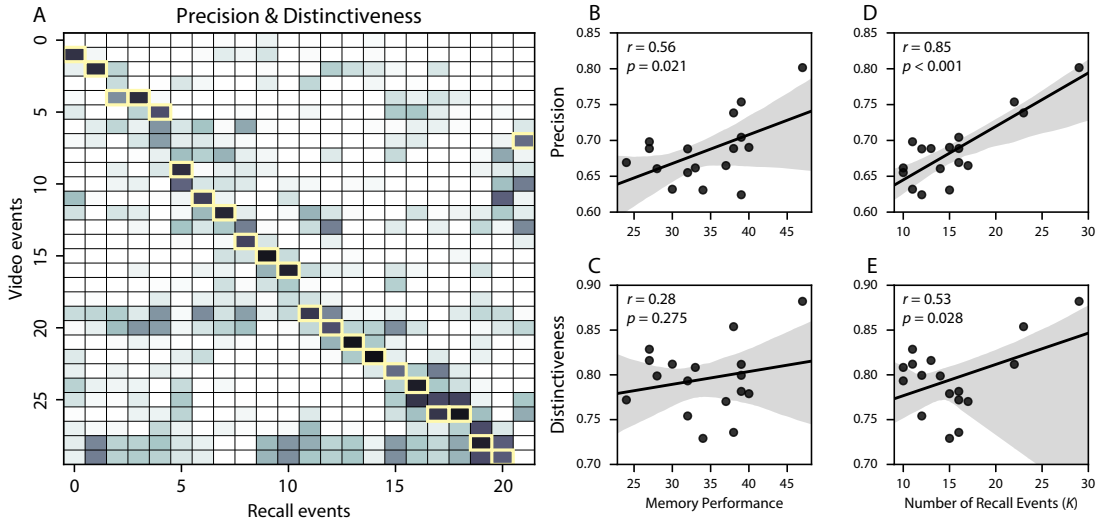


Figure 4: Novel content-based metrics of naturalistic memory: precision and distinctiveness. **A.** A video-recall correlation matrix for a representative participant (17). The yellow boxes highlight the maximum correlation in each column. Precision was computed as the average of the maximum correlation in each column. On the other hand, distinctiveness was defined as the average of everything except for the maximum correlation in each column. **B.** The (Pearson's) correlation between precision and hand-annotated memory performance. **C.** The correlation between precision and the number of events recovered by the model (k). **D.** The correlation between distinctiveness and hand-annotated memory performance. **E.** The correlation between distinctiveness and the number of events recovered by the model (k).

(Pearson's $r(15) = 0.56, p = 0.021$) and the number of recall events estimated by our model (Pearson's $r(15) = 0.85, p < 0.001$). A second novel metric we introduce here is distinctiveness, or how unique the recall description was to each video event. We define distinctiveness as 1 minus the average of all non-matching recall events from the video-recall correlation matrix. We hypothesized that participants who recounted events in a more distinctive way would display better overall memory. We find that this distinctiveness score is related to our model's estimated number of recalled events (Pearson's $r(15) = 0.49, p = 0.046$) but not to the analogous hand-annotated metric (Pearson's $r(15) = 0.31, p = 0.23$). In summary, using two novel metrics afforded by our approach, we find that participants whose recalls are both more precise and distinct remember more content.

The prior analyses leverage the correspondence between the 100-dimensional topic proportion matrices for the video and participants' recalls to characterize recall. However, it is difficult to gain

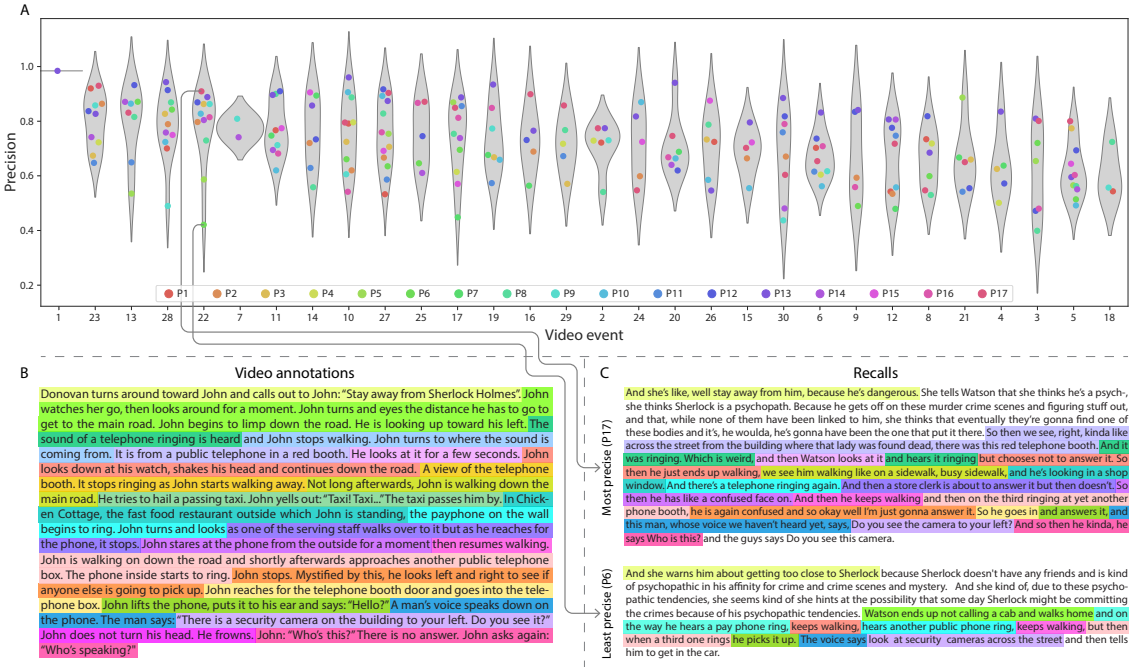


Figure 5: Precision metric reflects completeness of recall. **A.** Recall precision distributions over participants, for each video event. Grey violin plots display kernel density estimates for the distribution of recall precision scores for a single video event. Colored dots within the violin plots represent individual participants' recall precision for that event. Video events are ordered along the x-axis by the average precision with which they were remembered. **B.** The set of "Narrative details" video annotations (generated by Chen et al., 2017) for scenes comprising an example video event (22) identified by the HMM. Each action or feature is highlighted in a different color. **C.** A subset of the sentences comprising the most precise (P17) and least precise (P6) participants' recalls of video event 22. Descriptions of specific actions or features reflecting those highlighted in panel B are highlighted in the corresponding color.

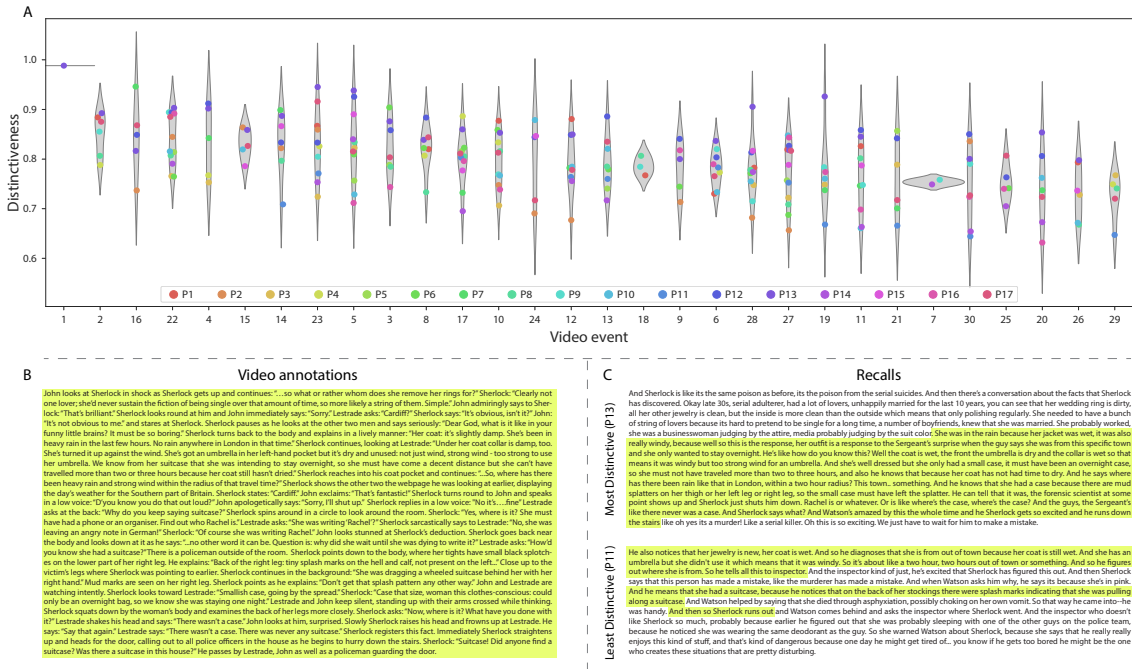


Figure 6: Distinctiveness metric reflects specificity of recall. A. Recall precision distributions over participants, for each video event. Grey violin plots display kernel density estimates for the distribution of recall precision scores for a single video event. Colored dots within the violin plots represent individual participants' recall precision for that event. Video events are ordered along the *x*-axis by the average precision with which they were remembered. B. The set of “Narrative details” video annotations (generated by Chen et al., 2017) for scenes comprising an example video event (22) identified by the HMM. Each action or feature is highlighted in a different color. C. A subset of the sentences comprising the most precise (P17) and least precise (P6) participants’ recalls of video event 22. Descriptions of specific actions or features reflecting those highlighted in panel B are highlighted in the corresponding color.

238 deep insights into that content solely by examining the topic proportion matrices (e.g., Figs. 2A,
239 D) or the corresponding correlation matrices (Figs. 2B, E, S4). To visualize the time-varying
240 high-dimensional content in a more intuitive way (Heusser et al., 2018b) we projected the topic
241 proportions matrices onto a two-dimensional space using Uniform Manifold Approximation and
242 Projection (UMAP; McInnes et al., 2018). In this lower-dimensional space, each point represents a
243 single video or recall event, and the distances between the points reflect the distances between the
244 events' associated topic vectors (Fig. 7). In other words, events that are near to each other in this
245 space are more semantically similar.

246 Visual inspection of the video and recall topic trajectories reveals a striking pattern. First,
247 the topic trajectory of the video (which reflects its dynamic content; Fig. 7A) is captured nearly
248 perfectly by the averaged topic trajectories of participants' recalls (Fig. 7B). To assess the consistency
249 of these recall trajectories across participants, we asked: given that a participant's recall trajectory
250 had entered a particular location in topic space, could the position of their *next* recalled event
251 be predicted reliably? For each location in topic space, we computed the set of line segments
252 connecting successively recalled events (across all participants) that intersected that location (see
253 *Methods* for additional details). We then computed (for each location) the distribution of angles
254 formed by the lines defined by those line segments and a fixed reference line (the *x*-axis). Rayleigh
255 tests revealed the set of locations in topic space at which these across-participant distributions
256 exhibited reliable peaks (blue arrows in Fig. 7B reflect significant peaks at $p < 0.05$, corrected). We
257 observed that the locations traversed by nearly the entire video trajectory exhibited such peaks.
258 In other words, participants exhibited similar trajectories that also matched the trajectory of the
259 original video (Fig. 7C). This is especially notable when considering the fact that the number of
260 events participants recalled (dots in Fig. 7C) varied considerably across people, and that every
261 participant used different words to describe what they had remembered happening in the video.
262 Differences in the numbers of remembered events appear in participants' trajectories as differences
263 in the sampling resolution along the trajectory. We note that this framework also provides a
264 means of detangling classic "proportion recalled" measures (i.e., the proportion of video events
265 referenced in participants' recalls) from participants' abilities to recapitulate the full shape of the

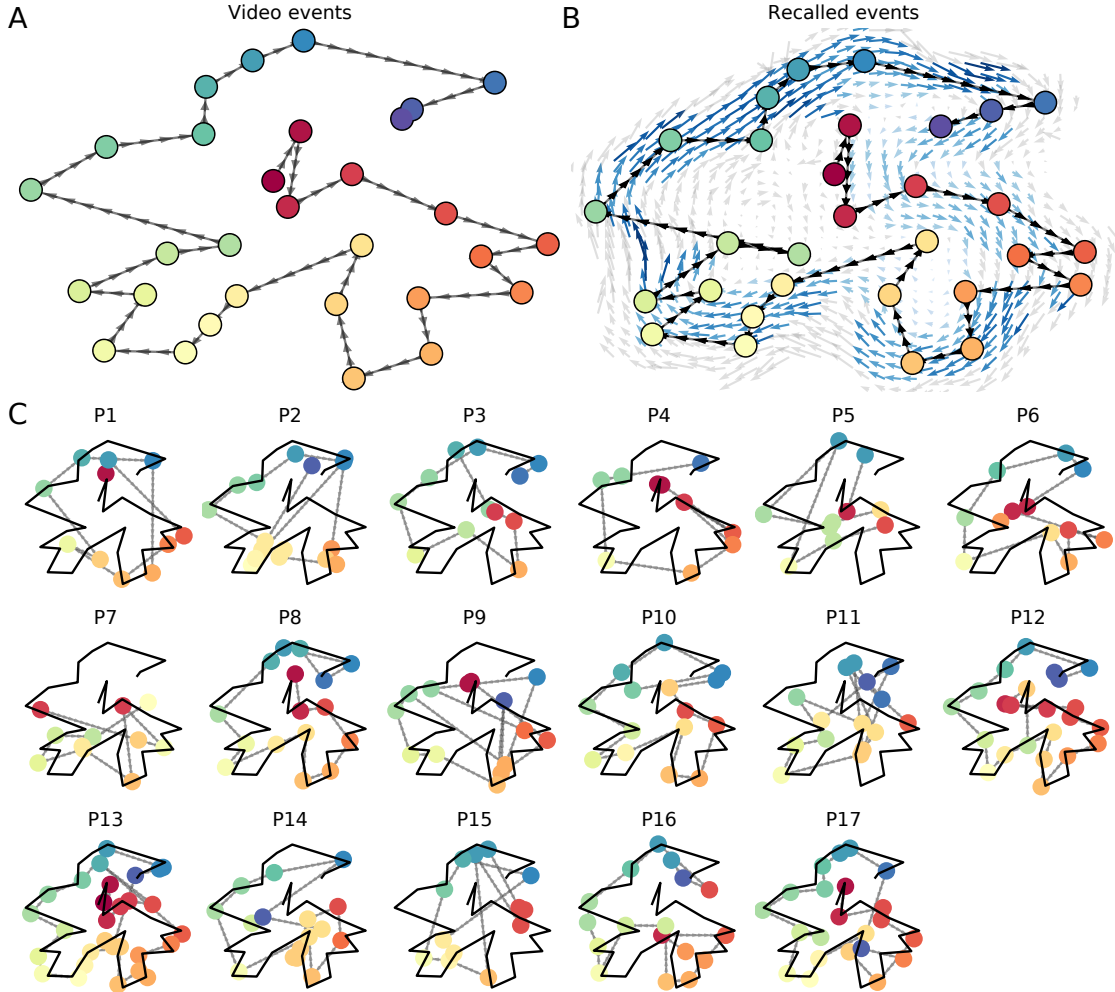


Figure 7: Trajectories through topic space capture the dynamic content of the video and recalls. All panels: the topic proportion matrices have been projected onto a shared two-dimensional space using UMAP. **A.** The two-dimensional topic trajectory taken by the episode of *Sherlock*. Each dot indicates an event identified using the HMM (see *Methods*); the dot colors denote the order of the events (early events are in red; later events are in blue), and the connecting lines indicate the transitions between successive events. **B.** The average two-dimensional trajectory captured by participants' recall sequences, with the same format and coloring as the trajectory in Panel A. To compute the event positions, we matched each recalled event with an event from the original video (see *Results*), and then we averaged the positions of all events with the same label. The arrows reflect the average transition direction through topic space taken by any participants whose trajectories crossed that part of topic space; blue denotes reliable agreement across participants via a Rayleigh test ($p < 0.05$, corrected). **C.** The recall topic trajectories (gray) taken by each individual participant (P1–P17). The video's trajectory is shown in black for reference. (Same format and coloring as Panel A.)

266 original video (i.e., the similarity in the shape of the original video trajectory and that defined by
267 each participant's recounting of the video).

268 Because our analysis framework projects the dynamic video content and participants' recalls
269 onto a shared topic space, and because the dimensions of that space are known (i.e., each topic
270 dimension is a set of weights over words in the vocabulary; Fig. S2), we can examine the topic
271 trajectories to understand which specific content was remembered well (or poorly). For each video
272 event, we can ask: what was the average correlation (across participants) between the video event's
273 topic vector and the closest matching recall event topic vectors from each participant? This yields
274 a single correlation coefficient for each video event, describing how closely participants' recalls of
275 the event tended to reliably capture its content (Fig. 8A). Given this summary of which events were
276 recalled reliably (or not), we next asked whether the better-remembered or worse-remembered
277 events tended to reflect particular topics. We computed a weighted average of the topic vectors for
278 each video event, where the weights reflected how reliably each event was recalled. To visualize
279 the result, we created a "wordle" image (Mueller et al., 2018) where words weighted more heavily
280 by better-remembered topics appear in a larger font (Fig. 8B, green box). Across the full video,
281 content that reflected topics necessary to convey the central focus of the video (e.g., the names of the
282 two main characters, "Sherlock" and "John", and the address of a major recurring location, "221B
283 Baker Street") were best remembered. An analogous analysis revealed which themes were poorly
284 remembered. Here in computing the weighted average over events' topic vectors, we weighted
285 each event in *inverse* proportion to how well it was remembered (Fig. 8B, red box). The least well-
286 remembered video content reflected information not necessary to conveying the video's "gist,"
287 such as the proper names of relatively minor characters (e.g., "Mike," "Molly," and "Lestrade")
288 and locations (e.g., "St. Bartholomew's Hospital"), as well as the brief, animated clip participants
289 viewed at the beginning of each of the two scan session (involving "singing" "cartoon" characters).

290 A similar result emerged from assessing the topic vectors for individual video and recall events
291 (Fig. 8C). Here, for each of the three best- and worst-remembered video events, we have constructed
292 two wordles: one from the original video event's topic vector (left) and a second from the average
293 recall topic vector for that event (right). The three best-remembered events (circled in green)

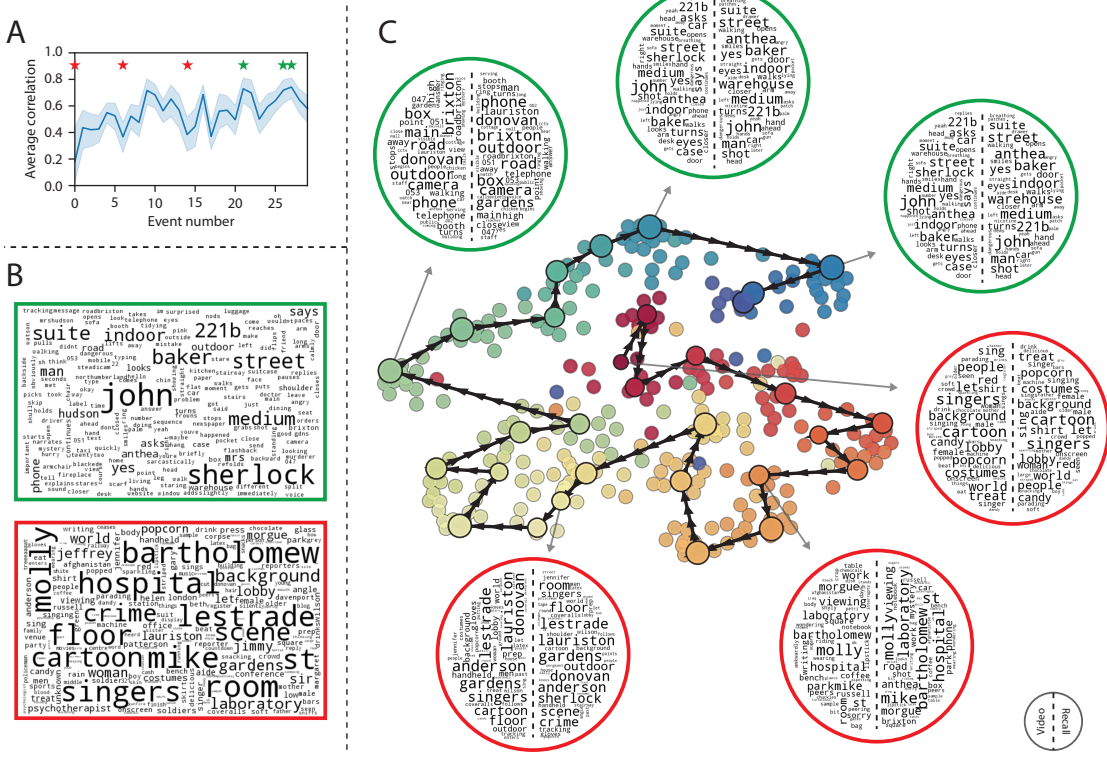


Figure 8: Transforming experience into memory. **A.** Average correlations (across participants) between the topic vectors from each video event and the closest-matching recall events. Error bars denote bootstrap-derived across-participant 95% confidence intervals. The stars denote the three best-remembered events (green) and worst-remembered events (red). **B.** Wordles comprising the top 200 highest-weighted words reflected in the weighted-average topic vector across video events. Green: video events were weighted by how well the topic vectors derived from recalls of those events matched the video events' topic vectors (Panel A). Red: video events were weighted by the inverse of how well their topic vectors matched the recalled topic vectors. **C.** The set of all video and recall events is projected onto the two-dimensional space derived in Figure 7. The dots outlined in black denote video events (dot size reflects the average correlation between the video event's topic vector and the topic vectors from the closest matching recalled events from each participant; bigger dots denote stronger correlations). The dots without black outlines denote recalled events. All dots are colored using the same scheme as Figure 7A. Wordles for several example events are displayed (green: three best-remembered events; red: three worst-remembered events). Within each circular wordle, the left side displays words associated with the topic vector for the video event, and the right side displays words associated with the (average) recall event topic vector, across all recall events matched to the given video event.

294 correspond to scenes important to the central plot-line: a mysterious figure spying on John in a
295 phone booth; John and Sherlock discussing the murders in their apartment; and Sherlock laying a
296 trap to catch the murderer. Meanwhile, the three worst-remembered events (circled in red) reflect
297 scenes that are non-essential to summarizing the narrative's structure: the two appearances of
298 singing cartoon characters; Molly watching as Sherlock beats a corpse in the morgue; and Sherlock
299 noticing evidence of Anderson's and Donovan's affair.

300 The results thus far inform us about which aspects of the dynamic content in the episode
301 participants watched were preserved or altered in participants' memories of the episode. We next
302 carried out a series of analyses aimed at understanding which brain structures might implement
303 these processes. In one analysis we sought to identify which brain structures were sensitive
304 to the video's dynamic content, as characterized by its topic trajectory. Specifically, we used a
305 searchlight procedure to identify the extent to which each cluster of voxels exhibited a timecourse
306 of activity (as the participants watched the video) whose temporal correlation matrix matched
307 the temporal correlation matrix of the original video's topic proportions (Fig. 2B). As shown
308 in Figure 10A, the analysis revealed a network of regions including bilateral frontal cortex and
309 cingulate cortex, suggesting that these regions may play a role in processing information relevant
310 to the narrative structure of the video. In a second analysis, we sought to identify which brain
311 structures' responses (while viewing the video) reflected how each participant would later *recall*
312 the video. We used an analogous searchlight procedure to identify clusters of voxels whose
313 temporal correlation matrices reflected the temporal correlation matrix of the topic proportions for
314 each individual's recalls (Figs. 2D, S4). As shown in Figure 10B, the analysis revealed a network of
315 regions including the ventromedial prefrontal cortex (vmPFC), anterior cingulate cortex (ACC), and
316 right medial temporal lobe (rMTL), suggesting that these regions may play a role in transforming
317 each individual's experience into memory. In identifying regions whose responses to ongoing
318 experiences reflect how those experiences will be remembered later, this latter analysis extends
319 classic *subsequent memory analyses* (e.g., Paller and Wagner, 2002) to domain of naturalistic stimuli.

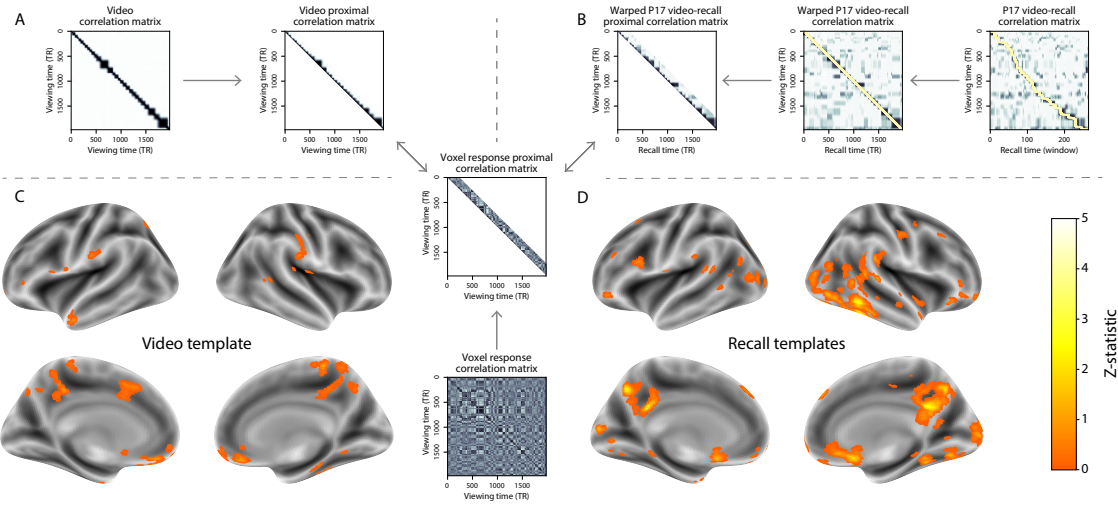


Figure 9: Brain structures that underlie the transformation of experience into memory. **A.** We searched for regions whose responses (as participants watched the video) matched the temporal correlation matrix of the video topic proportions. These regions are sensitive to the narrative structure of the video. **B.** We searched for regions whose responses (as participants watched the video) matched the temporal correlation matrix of the topic proportions derived from each individual's later recall of video. These regions are sensitive to how the narrative structure of the video is transformed into a memory of the video. Both panels: the maps are thresholded at $p < 0.05$, corrected.

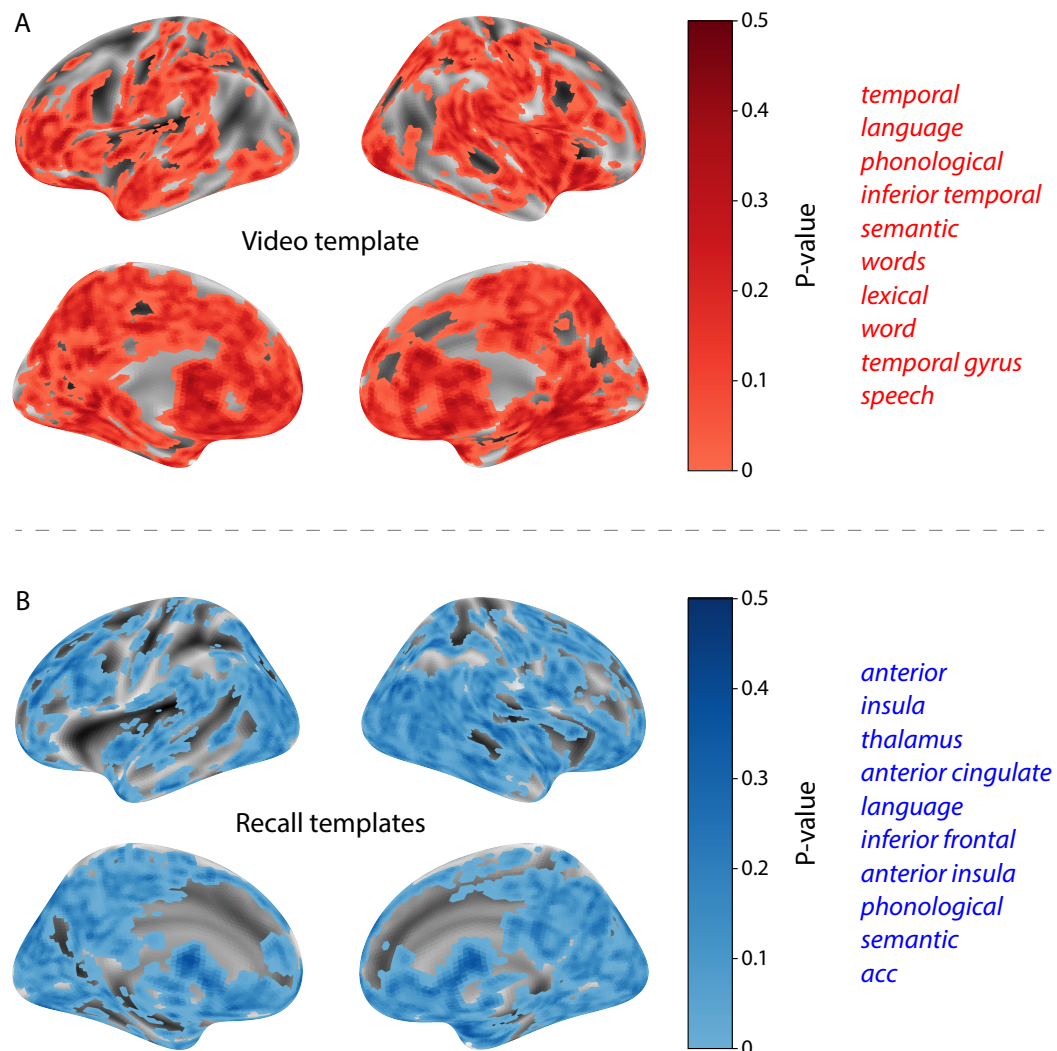


Figure 10: INSERT CAPTION HERE

320 **Discussion**

321 Our work casts remembering as reproducing (behaviorally and neurally) the topic trajectory, or
322 shape, of an experience. This view draws inspiration from prior work aimed at elucidating
323 the neural and behavioral underpinnings of how we process dynamic naturalistic experiences
324 and remember them later. One approach to identifying neural responses to naturalistic stimuli
325 (including experiences) entails building a model of the stimulus and searching for brain regions
326 whose responses are consistent with the model. In prior work, a series of studies from Uri
327 Hasson's group (Lerner et al., 2011; Simony et al., 2016; Chen et al., 2017; Baldassano et al., 2017;
328 Zadbood et al., 2017) have extended this approach with a clever twist: rather than building an
329 explicit stimulus model, these studies instead search for brain responses (while experiencing the
330 stimulus) that are reliably similar across individuals. So called *inter-subject correlation* (ISC) and
331 *inter-subject functional connectivity* (ISFC) analyses effectively treat other people's brain responses
332 to the stimulus as a "model" of how its features change over time. By contrast, in our present
333 work we used topic models and HMMs to construct an explicit stimulus model (i.e., the topic
334 trajectory of the video). When we searched for brain structures whose responses are consistent
335 with the video's topic trajectory, we identified a network of structures that overlapped strongly
336 with the "long temporal receptive window" network reported by the Hasson group (e.g., compare
337 our Fig. 10A with the map of long temporal receptive window voxels in Lerner et al., 2011). This
338 provides support for the notion that part of the long temporal receptive window network may be
339 maintaining an explicit model of the stimulus dynamics. When we performed a similar analysis
340 after swapping out the video's topic trajectory with the recall topic trajectories of each individual
341 participant, this allowed us to identify brain regions whose responses (as the participants viewed
342 the video) reflected how the video trajectory would be transformed in memory (as reflected by
343 the recall topic trajectories). The analysis revealed that the rMTL and vmPFC may play a role in
344 this person-specific transformation from experience into memory. The role of the MTL in episodic
345 memory encoding has been well-reported (e.g., Paller and Wagner, 2002; Davachi et al., 2003;
346 Ranganath et al., 2004; Davachi, 2006; Wiltgen and Silva, 2007; Diana et al., 2007; van Kesteren

347 et al., 2013). Prior work has also implicated the medial prefrontal cortex in representing “schema”
348 knowledge (i.e., general knowledge about the format of an ongoing experience given prior similar
349 experiences; van Kesteren et al., 2012, 2013; Schlichting and Preston, 2015; Gilboa and Marlatte,
350 2017; Spalding et al., 2018). Integrating across our study and this prior work, one interpretation is
351 that the person-specific transformations mediated (or represented) by the rMTL and vmPFC may
352 reflect schema knowledge being leveraged, formed, or updated, incorporating ongoing experience
353 into previously acquired knowledge.

354 In extending classical free recall analyses to our naturalistic memory framework, we recovered
355 two patterns of recall dynamics central to list-learning studies: a high probability of initiating
356 recall with the first video event (Fig. 3A) and a strong bias toward transitioning from recalling a
357 given event to recalling the event immediately following it (Fig. 3B). However, equally noteworthy
358 are the typical free recall results not recovered in these analyses, as each highlights a fundamental
359 difference between list-learning studies and naturalistic memory paradigms like the one employed
360 in the present study. The most noticeable departure from hallmark free recall dynamics in these
361 findings is the apparent lack of a serial position effect in Figure 3C, which instead shows greater
362 and lesser recall probabilities for events distributed across the video stimulus. Stimuli in free recall
363 experiments most often comprise lists of simple, common words, presented to participants in a
364 random order. (In fact, numerous word pools have been developed based on these criteria; e.g.,
365 Friendly et al., 1982). These stimulus qualities enable two assumptions that are central to word
366 list analyses, but frequently do not hold for real-world experiences. First, researchers conducting
367 free recall studies may assume that the content at each presentation index is essentially equal, and
368 does not bear qualities that would cause participants to remember it more or less successfully than
369 others. Such is rarely the case with real-world experiences or experiments meant to approximate
370 them, and the effects of both intrinsic and observer-dependent factors on stimulus memorability
371 are well established (for review see Chun and Turk-Browne, 2007; Bylinskii et al., 2015; Tyng
372 et al., 2017). Second, the random ordering of list items ensures that (across participants, on
373 average) there is no relationship between the thematic similarity of individual stimuli and their
374 presentation positions—in other words, two semantically related words are no more likely to be

375 presented next to each other than at opposite ends of the list. In most cases, the exact opposite
376 is true of real-world episodes. Our internal thoughts, our actions, and the physical state of the
377 world around us all tend to follow a direct, causal progression. As a result, each moment of our
378 experience tends to be inherently more similar to surrounding moments than to those in the distant
379 past or future. Memory literature has termed this strong temporal autocorrelation “context,” and
380 in various media that depict real-world events (e.g., movies and written stories), we recognize
381 it as a *narrative structure*. While a random word list (by definition) has no such structure, the
382 logical progression between ideas and actions in a naturalistic stimulus prompts the rememberer
383 to recount presented events in order, starting with the beginning. This tendency is reflected in our
384 findings’ second departure from typical free recall dynamics: a lack of increased probability of first
385 recall for end-of-sequence events (Fig. 3A).

386 Thus, analyses such as those in Figure 3 that address only the temporal dynamics of free re-
387 call paint an incomplete picture of memory for naturalistic episodes. While useful for studying
388 presentation order-dependent recall dynamics, they neglect to consider the stimuli’s content (or,
389 for example, that content’s potential interrelatedness). However, sensitivity to stimulus and recall
390 content introduces a new challenge: distinguishing between levels of recall quality for a stimulus
391 (i.e., an event) that is considered to have been “remembered.” When modeling memory experi-
392 ments, often times events (or items) and their later memories are treated as binary and independent
393 events (e.g., a given list item was simply either remembered or not remembered). Various models
394 of memory (e.g., Yonelinas, 2002) attempt to improve upon this by including confidence ratings,
395 rendering this binary judgement instead categorical. Our novel framework allows one to assess
396 memory performance in a more continuous way (*precision*), as well as analyze the correlational
397 structure of each encoding event to each memory event (*distinctiveness*). Further and importantly,
398 these two novel metrics we introduce here arise from comparisons of the actual content of the
399 experience/memories, which is not typically modeled. Leveraging this, we find that the successful
400 memory performance is related to 1) the precision with which the participant recounts each event
401 and 2) the distinctiveness of each recall event (relative to the other recalled events). The first finding
402 suggests that the information retained for *any individual event* may predict the overall amount of

403 information retained by the participant. The second finding suggests that the ability to distin-
404 guish between temporally or semantically similar content is also related to the quantity of content
405 recovered. Intriguingly, prior studies show that pattern separation, or the ability to discriminate
406 between similar experiences, is impaired in many cognitive disorders as well as natural aging
407 (Stark et al., 2010; Yassa et al., 2011; Yassa and Stark, 2011). Future work might explore whether
408 and how these metrics compare between cognitively impoverished groups and healthy controls.

409 While a large number of language models exist (e.g., WAS, LSA, word2vec, universal sentence
410 encoder; Steyvers et al., 2004; Landauer et al., 1998; Mikolov et al., 2013; Cer et al., 2018), here
411 we use latent dirichlet allocation (LDA)-based topic models for a few reasons. First, topic models
412 capture the *essence* of a text passage devoid of the specific set and order of words used. This
413 was an important feature of our model since different people may accurately recall a scene using
414 very different language. Second, words can mean different things in different contexts (e.g. “bat”
415 as the act of hitting a baseball, the object used for that action, or as a flying mammal). Topic
416 models are robust to this, allowing words to exist as part of multiple topics. Last, topic models
417 provide a straightforward means to recover the weights for the particular words comprising a topic,
418 enabling easy interpretation of an event’s contents (e.g. Fig. 8). Other models such as Google’s
419 universal sentence encoder offer a context-sensitive encoding of text passages, but the encoding
420 space is complex and non-linear, and thus recovering the original words used to fit the model is
421 not straightforward. However, it’s worth pointing out that our framework is divorced from the
422 particular choice of language model. Moreover, many of the aspects of our framework could be
423 swapped out for other choices. For example, the language model, the timeseries segmentation
424 model and the video-recall matching function could all be customized for the particular problem.
425 Indeed for some problems, recovery of the particular recall words may not be necessary, and thus
426 other text-modeling approaches (such as universal sentence encoder) may be preferable. Future
427 work will explore the influence of particular model choices on the framework’s accuracy.

428 Our work has broad implications for how we characterize and assess memory in real-world
429 settings, such as the classroom or physician’s office. For example, the most commonly used
430 classroom evaluation tools involve simply computing the proportion of correctly answered exam

431 questions. Our work indicates that this approach is only loosely related to what educators might
432 really want to measure: how well did the students understand the key ideas presented in the
433 course? Under this typical framework of assessment, the same exam score of 50% could be
434 ascribed to two very different students: one who attended the full course but struggled to learn
435 more than a broad overview of the material, and one who attended only half of the course but
436 understood the material perfectly. Instead, one could apply our computational framework to build
437 explicit content models of the course material and exam questions. This approach would provide
438 a more nuanced and specific view into which aspects of the material students had learned well
439 (or poorly). In clinical settings, memory measures that incorporate such explicit content models
440 might also provide more direct evaluations of patients' memories.

441 **Methods**

442 **Experimental design and data collection**

443 Data were collected by Chen et al. (2017). In brief, participants ($n = 17$) viewed the first 48 minutes
444 of "A Study in Pink", the first episode of the BBC television series *Sherlock*, while fMRI volumes
445 were collected (TR = 1500 ms). The stimulus was divided into a 23 min (946 TR) and a 25 min
446 (1030 TR) segment to mitigate technical issues related to the scanner. After finishing the clip,
447 participants were instructed to (quoting from Chen et al., 2017) "describe what they recalled of the
448 [episode] in as much detail as they could, to try to recount events in the original order they were
449 viewed in, and to speak for at least 10 minutes if possible but that longer was better. They were told
450 that completeness and detail were more important than temporal order, and that if at any point
451 they realized they had missed something, to return to it. Participants were then allowed to speak
452 for as long as they wished, and verbally indicated when they were finished (e.g., 'I'm done')."
453 For additional details about the experimental procedure and scanning parameters, see Chen et al.
454 (2017). The experimental protocol was approved by Princeton University's Institutional Review
455 Board.

456 After preprocessing the fMRI data and warping the images into a standard (3 mm³ MNI) space,
457 the voxel activations were z-scored (within voxel) and spatially smoothed using a 6 mm (full width
458 at half maximum) Gaussian kernel. The fMRI data were also cropped so that all video-viewing
459 data were aligned across participants. This included a constant 3 TR (4.5 s) shift to account for the
460 lag in the hemodynamic response. (All of these preprocessing steps followed Chen et al., 2017,
461 where additional details may be found.)

462 **Data and code availability**

463 The fMRI data we analyzed are available online [here](#). The behavioral data and all of our analysis
464 code may be downloaded [here](#).

465 **Statistics**

466 All statistical tests we performed were two-sided.

467 **Modeling the dynamic content of the video and recall transcripts**

468 **Topic modeling**

469 The input to the topic model we trained to characterize the dynamic content of the video comprised
470 998 hand-generated annotations of short (mean: 2.96s) scenes spanning the video clip (Chen et al.,
471 2017 generated 1000 annotations total; we removed two referring to the break between the first and
472 second scan sessions, during which no fMRI data was collected). The features annotated included:
473 narrative details (a sentence or two describing what happened in that scene); whether the scene
474 took place indoors or outdoors; names of any characters that appeared in the scene; name(s) of
475 characters in camera focus; name(s) of characters who were speaking in the scene; the location (in
476 the story) that the scene took place; camera angle (close up, medium, long, top, tracking, over the
477 shoulder, etc.); whether music was playing in the scene or not; and a transcription of any on-screen
478 text. We concatenated the text for all of these features within each segment, creating a “bag of
479 words” describing each scene. We then re-organized the text descriptions into overlapping sliding

480 windows of 50 scenes each. In other words, we created a “context” for each scene comprising the
481 text descriptions of the preceding 25 scenes, the present scene, and the following 24 scenes. To
482 model the “context” at the beginning and end of the video (i.e., within 25 scenes of the beginning or
483 end), we created overlapping sliding windows that grew in size from one scene to the full length,
484 then similarly tapered their length at the end. This bore the additional benefit of representing each
485 scene’s description in the text corpus an equal number of times.

486 We trained our model using these overlapping text samples with `scikit-learn` (version 0.19.1;
487 Pedregosa et al., 2011), called from our high-dimensional visualization and text analysis software,
488 `HyperTools` (Heusser et al., 2018b). Specifically, we used the `CountVectorizer` class to transform
489 the text from each window into a vector of word counts (using the union of all words across all
490 scenes as the “vocabulary,” excluding English stop words); this yielded a number-of-windows
491 by number-of-words *word count* matrix. We then used the `LatentDirichletAllocation` class
492 (`topics=100, method='batch'`) to fit a topic model (Blei et al., 2003) to the word count matrix,
493 yielding a number-of-windows (1047) by number-of-topics (100) *topic proportions* matrix. The
494 topic proportions matrix describes which mix of topics (latent themes) is present in and around
495 each scene. Next, we transformed the topic proportions matrix to match the 1976 fMRI volume
496 acquisition times. We assigned each topic vector to the timepoint midway between the beginning
497 of the first scene and the end of the last scene in its corresponding sliding text window. We
498 then transformed these timepoints to units of TRs and interpolated the dynamic topic proportions
499 matrix to obtain number-of-TRs (1976) by number-of-topics (100) matrix.

500 We created similar topic proportions matrices using hand-annotated transcripts of each partici-
501 pant’s recall of the video (annotated by Chen et al., 2017). We tokenized the transcript into a list of
502 sentences, and then re-organized the list into overlapping sliding windows spanning 10 sentences
503 each (and analogously tapered the lengths of the first and last 10 sliding windows). In turn, we
504 transformed each window’s sentences into a word count vector (using the same vocabulary as for
505 the video model). We then used the topic model already trained on the video scenes to compute
506 the most probable topic proportions for each sliding window. This yielded a number-of-windows
507 (range: 83–312) by number-of-topics (100) topic proportions matrix for each participant. These

508 reflected the dynamic content of each participant's recalls. Note: for details on how we selected the
509 video and recall window lengths and number of topics, see *Supporting Information* and Figure S1.

510 **Parsing topic trajectories into events using Hidden Markov Models**

511 We parsed the topic trajectories of the video and participants' recalls into events using Hidden
512 Markov Models (Rabiner, 1989). Given the topic proportions matrix (describing the mix of topics
513 at each timepoint) and a number of states, K , an HMM recovers the set of state transitions that
514 segments the timeseries into K discrete states. Following Baldassano et al. (2017), we imposed an
515 additional set of constraints on the discovered state transitions that ensured that each state was
516 encountered exactly once (i.e., never repeated). We used the BrainIAK toolbox (Capota et al., 2017)
517 to implement this segmentation.

518 We used an optimization procedure to select the appropriate K for each topic proportions
519 matrix. Prior studies on narrative structure and processing have shown that we both perceive
520 and internally represent the world around us at multiple, hierarchical timescales (e.g., Hasson
521 et al., 2008; Lerner et al., 2011; Hasson et al., 2015; Chen et al., 2017; Baldassano et al., 2017, 2018).
522 However, for the purposes of our framework, we sought to identify the single timescale of event-
523 representations that is emphasized *most heavily* in the temporal structure of the video and each
524 participant's recalls. We quantified this as the set of K event boundaries that yielded the maximal
525 distinctiveness between the content (i.e., topics) within each event and that in all other events.
526 Specifically, we computed (for each matrix)

$$\operatorname{argmax}_K [W_1(a, b)],$$

527 where a was the distribution of correlations between the topic vectors of timepoints within the
528 same state and b was the average correlation between the topic vectors of timepoints within
529 *different* states. For each possible K , we computed the first Wasserstein distance (W_1 ; also known as
530 "earth mover's distance"; Dobrushin, 1970; Ramdas et al., 2017) between these distributions, and
531 chose the K -value that yielded the greatest difference. Figure 2B displays the event boundaries

532 returned for the video, and Figure S4 displays the event boundaries returned for each participant's
533 recalls (See Fig. S6 for the optimization functions for the video and recalls). After obtaining these
534 event boundaries, we created stable estimates of each topic proportions matrix by averaging the
535 topic vectors within each event. This yielded a number-of-events by number-of-topics matrix for
536 the video and recalls from each participant.

537 **Naturalistic extensions of classic list-learning analyses**

538 In traditional list-learning experiments, participants view a list of items (e.g., words) and then recall
539 the items later. Our video-recall event matching approach affords us the ability to analyze memory
540 in a similar way. The video and recall events can be treated analogously to studied and recalled
541 "items" in a list-learning study. We can then extend classic analyses of memory performance and
542 dynamics (originally designed for list-learning experiments) to the more naturalistic video recall
543 task used in this study.

544 Perhaps the simplest and most widely used measure of memory performance is *accuracy*—i.e.,
545 the proportion of studied (experienced) items (in this case, the 30 video events) that the participant
546 later remembered. Chen et al. (2017) developed a human rating system whereby the quality of
547 each participant's memory was evaluated by an independent rater. We found a strong across-
548 participants correlation between these independant ratings and the overall number of events that
549 our HMM approach identified in participants' recalls (Pearson's $r(15) = 0.65, p = 0.004$).

550 As described below, we next considered a number of memory performance measures that are
551 typically associated with list-learning studies. We also provide a software package, Quail, for
552 carrying out these analyses (Heusser et al., 2017).

553 **Probability of first recall (PFR).** PFR curves (Welch and Burnett, 1924; Postman and Phillips,
554 1965; Atkinson and Shiffrin, 1968) reflect the probability that an item will be recalled first as a
555 function of its serial position during encoding. To carry out this analysis, we initialized a number-
556 of-participants (17) by number-of-video-events (30) matrix of zeros. Then for each participant, we
557 found the index of the video event that was recalled first (i.e., the video event whose topic vector

558 was most strongly correlated with that of the first recall event) and filled in that index in the matrix
559 with a 1. Finally, we averaged over the rows of the matrix, resulting in a 1 by 30 array representing
560 the proportion of participants that recalled an event first, as a function of the order of the event's
561 appearance in the video (Fig. 3A).

562 **Lag conditional probability curve (lag-CRP).** The lag-CRP curve (Kahana, 1996) reflects the
563 probability of recalling a given event after the just-recalled event, as a function of their relative
564 positions (or *lag*). In other words, a lag of 1 indicates that a recalled event came immediately after
565 the previously recalled event in the video, and a lag of -3 indicates that a recalled event came 3
566 events before the previously recalled event. For each recall transition (following the first recall),
567 we computed the lag between the current recall event and the next recall event, normalizing by
568 the total number of possible transitions. This yielded a number-of-participants (17) by number-
569 of-lags (-29 to +29; 61 lags total) matrix. We averaged over the rows of this matrix to obtain a
570 group-averaged lag-CRP curve (Fig. 3B).

571 **Serial position curve (SPC).** SPCs (Murdock, 1962) reflect the proportion of participants that
572 remember each item as a function of the items' serial position during encoding. We initialized
573 a number-of-participants (17) by number-of-video-events (30) matrix of zeros. Then, for each
574 recalled event, for each participant, we found the index of the video event that the recalled event
575 most closely matched (via the correlation between the events' topic vectors) and entered a 1 into
576 that position in the matrix (i.e., for the given participant and event). This resulted in a matrix
577 whose entries indicated whether or not each event was recalled by each participant (depending
578 on whether the corresponding entires were set to one or zero). Finally, we averaged over the rows
579 of the matrix to yield a 1 by 30 array representing the proportion of participants that recalled each
580 event as a function of the order of the event's appearance in the video (Fig. 3C).

581 **Temporal clustering scores.** Temporal clustering describes participants' tendency to organize
582 their recall sequences by the learned items' encoding positions. For instance, if a participant
583 recalled the video events in the exact order they occurred (or in exact reverse order), this would

584 yield a score of 1. If a participant recalled the events in random order, this would yield an expected
585 score of 0.5. For each recall event transition (and separately for each participant), we sorted
586 all not-yet-recalled events according to their absolute lag (i.e., distance away in the video). We
587 then computed the percentile rank of the next event the participant recalled. We averaged these
588 percentile ranks across all of the participant’s recalls to obtain a single temporal clustering score
589 for the participant.

590 **Semantic clustering scores.** Semantic clustering describes participants’ tendency to recall seman-
591 tically similar presented items together in their recall sequences. Here, we used the topic vectors
592 for each event as a proxy for its semantic content. Thus, the similarity between the semantic
593 content for two events can be computed by correlating their respective topic vectors. For each
594 recall event transition, we sorted all not-yet-recalled events according to how correlated the topic
595 vector of *the closest-matching video event* was to the topic vector of the closest-matching video event
596 to the just-recalled event. We then computed the percentile rank of the observed next recall. We
597 averaged these percentile ranks across all of the participant’s recalls to obtain a single semantic
598 clustering score for the participant.

599 **Novel naturalistic memory metrics**

600 **Precision.** We tested whether participants who recalled more events were also more *precise* in
601 their recollections. For each participant, we computed the average correlation between the topic
602 vectors for each recall event and those of its closest-matching video event. This gave a single value
603 per participant representing the average precision across all recalled events. We then Fisher’s *z*-
604 transformed these values and correlated them with both hand-annotated and model-derived (i.e.,
605 k or the number of events recovered by the HMM) memory performance.

606 **Distinctiveness.** We also considered the *distinctiveness* of each recalled event. That is, how
607 uniquely a recalled event’s topic vector matched a given video event topic vector, versus the
608 topic vectors for the other video events. We hypothesized that participants with high memory

609 performance might describe each event in a more distinctive way (relative to those with lower
610 memory performance who might describe events in a more general way). To test this hypothesis
611 we define a distinctiveness score for each recall event as

$$d(\text{event}) = 1 - \bar{c}(\text{event}),$$

612 where $\bar{c}(\text{event})$ is the average correlation between the given recalled event's topic vector and the
613 topic vectors from all video events *except* the best-matching video event. We then averaged these
614 distinctiveness scores across all of the events recalled by the given participant. As above, we used
615 Fisher's *z*-transformation before correlating these values with hand-annotated and model derived
616 memory performance scores across-subjects.

617 **Visualizing the video and recall topic trajectories**

618 We used the UMAP algorithm (McInnes et al., 2018) to project the 100-dimensional topic space
619 onto a two-dimensional space for visualization (Figs. 7, 8). Importantly, to ensure that all of
620 the trajectories were projected onto the *same* lower dimensional space, we computed the low-
621 dimensional embedding on a "stacked" matrix created by vertically concatenating the events-
622 by-topics topic proportions matrices for the video, across-participants average recalls and all 17
623 individual participants' recalls. We then divided the rows of the result (a total-number-of-events
624 by two matrix) back into separate matrices for the video topic trajectory and the trajectories for
625 each participant's recalls (Fig. 7). This general approach for discovering a shared low-dimensional
626 embedding for a collections of high-dimensional observations follows Heusser et al. (2018b). Note:
627 for further details on how we created this low-dimensional embedding space, see *Supporting
628 Information*.

629 **Estimating the consistency of flow through topic space across participants**

630 In Figure 7B, we present an analysis aimed at characterizing locations in topic space that dif-
631 ferent participants move through in a consistent way (via their recall topic trajectories). The

632 two-dimensional topic space used in our visualizations (Fig. 7) comprised a 60×60 (arbitrary
633 units) square. We tiled this space with a 50×50 grid of evenly spaced vertices, and defined a
634 circular area centered on each vertex whose radius was two times the distance between adjacent
635 vertices (i.e., 2.4 units). For each vertex, we examined the set of line segments formed by connecting
636 each pair successively recalled events, across all participants, that passed through this circle. We
637 computed the distribution of angles formed by those segments and the x -axis, and used a Rayleigh
638 test to determine whether the distribution of angles was reliably “peaked” (i.e., consistent across
639 all transitions that passed through that local portion of topic space). To create Figure 7B we drew
640 an arrow originating from each grid vertex, pointing in the direction of the average angle formed
641 by line segments that passed within its circular radius. We set the arrow lengths to be inversely
642 proportional to the p -values of the Rayleigh tests at each vertex. Specifically, for each vertex we
643 converted all of the angles of segments that passed within 2.4 units to unit vectors, and we set
644 the arrow lengths at each vertex proportional to the length of the (circular) mean vector. We also
645 indicated any significant results ($p < 0.05$, corrected using the Benjamani-Hochberg procedure) by
646 coloring the arrows in blue (darker blue denotes a lower p -value, i.e., a longer mean vector); all
647 tests with $p \geq 0.05$ are displayed in gray and given a lower opacity value.

648 **Searchlight fMRI analyses**

649 In Figure 10, we present two analyses aimed at identifying brain regions whose responses (as par-
650 ticipants viewed the video) exhibited a particular temporal structure. We developed a searchlight
651 analysis wherein we constructed a cube centered on each voxel (radius: 5 voxels) and for each
652 of these cubes, computed the temporal correlation matrix of the voxel responses during video
653 viewing. Specifically, for each of the 1976 volumes collected during video viewing, we correlated
654 the activity patterns in the given cube with the activity patterns (in the same cube) collected during
655 every other timepoint. This yielded a 1976 by 1976 correlation matrix for each cube.

656 Next, we constructed a series of “template” matrices: the first reflecting the timecourse of
657 video’s topic trajectory, and the others reflecting that of each participant’s recall topic trajectory.
658 To construct the video template, we computed the correlations between the topic proportions

estimated for every pair of TRs (prior to segmenting the trajectory into discrete events; i.e., the correlation matrix shown in Figs. 2B and 10A). We constructed similar temporal correlation matrices for each participant's recall topic trajectory (Figs. 2D, S4). However, to correct for length differences and potential non-linear transformations between viewing time and recall time, we first used dynamic time warping (Berndt and Clifford, 1994) to temporally align participants' recall topic trajectories with the video topic trajectory. An example correlation matrix before and after warping is shown in Fig. 10B. This yielded a 1976 by 1976 correlation matrix for the video template and for each participant's recall template.

To determine which (cubes of) voxel responses matched the video template, we correlated the upper triangle of the voxel correlation matrix for each cube with the upper triangle of the video template matrix (Kriegeskorte et al., 2008). This yielded, for each participant, a voxelwise map of correlation values. We then performed a one-sample *t*-test on the distribution of (Fisher *z*-transformed) correlations at each voxel, across participants. This resulted in a value for each voxel (cube), describing how reliably its timecourse mirrored that of the video.

We further sought to ensure that our analysis identified regions where the activations' temporal structure specifically reflected that of the video, rather than regions whose activity was simply autocorrelated at a width similar to the video template's diagonal. To achieve this, we used a phase shift-based permutation procedure, wherein we circularly shifted the video's topic trajectory by a random number of timepoints, computed the resulting "null" video template, and re-ran the searchlight analysis, in full. (For each of the 100 permutations, the same random shift was used for all participants). We *z*-scored the observed (unshifted) result at each voxel against the distribution of permutation-derived "null" results, and estimated a *p*-value by computing the proportion of shifted results that yielded larger values. To create the map in Figure 10A, we thresholded out any voxels whose similarity to the unshifted video's structure fell below the 95th percentile of the permutation-derived similarity results.

We used an analogous procedure to identify which voxels' responses reflected the recall templates. For each participant, we correlated the upper triangle of the correlation matrix for each cube of voxels with their (time warped) recall correlation matrix. As in the video template analysis this

687 yielded a voxelwise map of correlation coefficients per participant. However, whereas the video
688 analysis compared every participant's responses to the same template, here the recall templates
689 were unique for each participant. As in the analysis described above, we *t*-scored the (Fisher
690 *z*-transformed) voxelwise correlations, and used the same permutation procedure we developed
691 for the video responses to ensure specificity to the recall timeseries and assign significance values.
692 To create the map in Figure 10B we again thresholded out any voxels whose correspondence values
693 fell below the 95th percentile of the permutation-derived null distribution.

694 References

- 695 Atkinson, R. C. and Shiffrin, R. M. (1968). Human memory: A proposed system and its control
696 processes. In Spence, K. W. and Spence, J. T., editors, *The psychology of learning and motivation*,
697 volume 2, pages 89–105. Academic Press, New York.
- 698 Baldassano, C., Chen, J., Zadbood, A., Pillow, J. W., Hasson, U., and Norman, K. A. (2017).
699 Discovering event structure in continuous narrative perception and memory. *Neuron*, 95(3):709–
700 721.
- 701 Baldassano, C., Hasson, U., and Norman, K. A. (2018). Representation of real-world event schemas
702 during narrative perception. *Journal of Neuroscience*, 38(45):9689–9699.
- 703 Berndt, D. J. and Clifford, J. (1994). Using dynamic time warping to find patterns in time series. In
704 *KDD workshop*, volume 10, pages 359–370.
- 705 Blei, D. M. and Lafferty, J. D. (2006). Dynamic topic models. In *Proceedings of the 23rd International
706 Conference on Machine Learning*, ICML '06, pages 113–120, New York, NY, US. ACM.
- 707 Blei, D. M., Ng, A. Y., and Jordan, M. I. (2003). Latent dirichlet allocation. *Journal of Machine
708 Learning Research*, 3:993 – 1022.
- 709 Brunec, I. K., Moscovitch, M. M., and Barense, M. D. (2018). Boundaries shape cognitive represen-
710 tations of spaces and events. *Trends in Cognitive Sciences*, 22(7):637–650.

- 711 Bylinskii, Z., Isola, P., Bainbridge, C., Torralba, A., and Oliva, A. (2015). Intrinsic and extrinsic
712 effects on image memorability. *Vision Research*, 116:165–178.
- 713 Capota, M., Turek, J., Chen, P.-H., Zhu, X., Manning, J. R., Sundaram, N., Keller, B., Wang, Y., and
714 Shin, Y. S. (2017). Brain imaging analysis kit.
- 715 Cer, D., Yang, Y., Kong, S. Y., Hua, N., Limtiaco, N., John, R. S., Constant, N., Guajardo-Cespedes,
716 M., Yuan, S., Tar, C., Sung, Y.-H., Strope, B., and Kurzweil, R. (2018). Universal sentence encoder.
717 *arXiv*, 1803.11175.
- 718 Chen, J., Leong, Y. C., Honey, C. J., Yong, C. H., Norman, K. A., and Hasson, U. (2017). Shared
719 memories reveal shared structure in neural activity across individuals. *Nature Neuroscience*,
720 20(1):115.
- 721 Chun, M. and Turk-Browne, N. (2007). Interactions between attention and memory. *Current opinion
722 in neurobiology*, 17(2):177–184.
- 723 Clewett, D. and Davachi, L. (2017). The ebb and flow of experience determines the temporal
724 structure of memory. *Curr Opin Behav Sci*, 17:186–193.
- 725 Davachi, L. (2006). Item, context and relational episodic encoding in humans. *Current Opinion in
726 Neurobiology*, 16(6):693—700.
- 727 Davachi, L., Mitchell, J. P., and Wagner, A. D. (2003). Multiple routes to memory: distinct medial
728 temporal lobe processes build item and source memories. *Proceedings of the National Academy of
729 Sciences, USA*, 100(4):2157 – 2162.
- 730 Diana, R. A., Yonelinas, A. P., and Ranganath, C. (2007). Imaging recollection and famil-
731 iarity in the medial temporal lobe: a three-component model. *Trends in Cognitive Sciences*,
732 doi:10.1016/j.tics.2007.08.001.
- 733 Dobrushin, R. L. (1970). Prescribing a system of random variables by conditional distributions.
734 *Theory of Probability & Its Applications*, 15(3):458–486.

- 735 DuBrow, S. and Davachi, L. (2013). The influence of contextual boundaries on memory for the
736 sequential order of events. *Journal of Experimental Psychology: General*, 142(4):1277–1286.
- 737 Ezzyat, Y. and Davachi, L. (2011). What constitutes an episode in episodic memory? *Psychological
738 Science*, 22(2):243–252.
- 739 Friendly, M., Franklin, P. E., Hoffman, D., and Rubin, D. C. (1982). The Toronto Word Pool:
740 Norms for imagery, concreteness, orthographic variables, and grammatical usage for 1,080
741 words. *Behavior Research Methods and Instrumentation*, 14:375–399.
- 742 Gilboa, A. and Marlatte, H. (2017). Neurobiology of schemas and schema-mediated memory.
743 *Trends Cogn Sci*, 21(8):618–631.
- 744 Hasson, U., Chen, J., and Honey, C. J. (2015). Hierarchical process memory: memory as an integral
745 component of information processing. *Trends in Cognitive Science*, 19(6):304–315.
- 746 Hasson, U., Yang, E., Vallines, I., Heeger, D. J., and Rubin, N. (2008). A hierarchy of temporal
747 receptive windows in human cortex. *Journal of Neuroscience*, 28(10):2539–2550.
- 748 Heusser, A. C., Ezzyat, Y., Shiff, I., and Davachi, L. (2018a). Perceptual boundaries cause mnemonic
749 trade-offs between local boundary processing and across-trial associative binding. *Journal of
750 Experimental Psychology Learning, Memory, and Cognition*, 44(7):1075–1090.
- 751 Heusser, A. C., Fitzpatrick, P. C., Field, C. E., Ziman, K., and Manning, J. R. (2017). Quail: a
752 Python toolbox for analyzing and plotting free recall data. *The Journal of Open Source Software*,
753 10.21105/joss.00424.
- 754 Heusser, A. C., Ziman, K., Owen, L. L. W., and Manning, J. R. (2018b). HyperTools: a Python
755 toolbox for gaining geometric insights into high-dimensional data. *Journal of Machine Learning
756 Research*, 18(152):1–6.
- 757 Howard, M. W. and Kahana, M. J. (2002). A distributed representation of temporal context. *Journal
758 of Mathematical Psychology*, 46:269–299.

- 759 Howard, M. W., MacDonald, C. J., Tiganj, Z., Shankar, K. H., Du, Q., Hasselmo, M. E., and H., E.
760 (2014). A unified mathematical framework for coding time, space, and sequences in the medial
761 temporal lobe. *Journal of Neuroscience*, 34(13):4692–4707.
- 762 Howard, M. W., Viskontas, I. V., Shankar, K. H., and Fried, I. (2012). Ensembles of human MTL
763 neurons “jump back in time” in response to a repeated stimulus. *Hippocampus*, 22:1833–1847.
- 764 Huk, A., Bonnen, K., and He, B. J. (2018). Beyond trial-based paradigms: continuous behavior, on-
765 going neural activity, and naturalistic stimuli. *Journal of Neuroscience*, 10.1523/JNEUROSCI.1920-
766 17.2018.
- 767 Kahana, M. J. (1996). Associative retrieval processes in free recall. *Memory & Cognition*, 24:103–109.
- 768 Koriat, A. and Goldsmith, M. (1994). Memory in naturalistic and laboratory contexts: distin-
769 guishing accuracy-oriented and quantity-oriented approaches to memory assessment. *Journal of*
770 *Experimental Psychology: General*, 123(3):297–315.
- 771 Kriegeskorte, N., Mur, M., and Bandettini, P. (2008). Representational similarity analysis – con-
772 necting the branches of systems neuroscience. *Frontiers in Systems Neuroscience*, 2:1 – 28.
- 773 Landauer, T. K., Foltz, P. W., and Laham, D. (1998). Introduction to latent semantic analysis.
774 *Discourse Processes*, 25:259–284.
- 775 Lerner, Y., Honey, C. J., Silbert, L. J., and Hasson, U. (2011). Topographic mapping of a hierarchy
776 of temporal receptive windows using a narrated story. *Journal of Neuroscience*, 31(8):2906–2915.
- 777 Manning, J. R. (2019). Episodic memory: mental time travel or a quantum ‘memory wave’ function?
778 *PsyArXiv*, doi:10.31234/osf.io/6zjwb.
- 779 Manning, J. R., Norman, K. A., and Kahana, M. J. (2015). The role of context in episodic memory.
780 In Gazzaniga, M., editor, *The Cognitive Neurosciences, Fifth edition*, pages 557–566. MIT Press.
- 781 Manning, J. R., Polyn, S. M., Baltuch, G., Litt, B., and Kahana, M. J. (2011). Oscillatory patterns
782 in temporal lobe reveal context reinstatement during memory search. *Proceedings of the National
783 Academy of Sciences, USA*, 108(31):12893–12897.

- 784 McInnes, L., Healy, J., and Melville, J. (2018). UMAP: Uniform manifold approximation and
785 projection for dimension reduction. *arXiv*, 1802(03426).
- 786 Mikolov, T., Chen, K., Corrado, G., and Dean, J. (2013). Efficient estimation of word representations
787 in vector space. *arXiv*, 1301.3781.
- 788 Mueller, A., Fillion-Robin, J.-C., Boidol, R., Tian, F., Nechifor, P., yoonsubKim, Peter, Rampin, R.,
789 Corvellec, M., Medina, J., Dai, Y., Petrushev, B., Langner, K. M., Hong, Alessio, Ozsvald, I.,
790 vkolmakov, Jones, T., Bailey, E., Rho, V., IgorAPM, Roy, D., May, C., foobuzz, Piyush, Seong,
791 L. K., Goey, J. V., Smith, J. S., Gus, and Mai, F. (2018). WordCloud 1.5.0: a little word cloud
792 generator in Python. *Zenodo*, <https://zenodo.org/record/1322068#.W4tPKZNKh24>.
- 793 Murdock, B. B. (1962). The serial position effect of free recall. *Journal of Experimental Psychology*,
794 64:482–488.
- 795 Paller, K. A. and Wagner, A. D. (2002). Observing the transformation of experience into memory.
796 *Trends in Cognitive Sciences*, 6(2):93–102.
- 797 Pedregosa, F., Varoquaux, G., Gramfort, A., Michel, V., Thirion, B., Grisel, O., Blondel, M., Pretten-
798 hofer, P., Weiss, R., Dubourg, V., Vanderplas, J., Passos, A., Cournapeau, D., Brucher, M., Perrot,
799 M., and Duchesnay, E. (2011). Scikit-learn: Machine learning in Python. *Journal of Machine
800 Learning Research*, 12:2825–2830.
- 801 Polyn, S. M., Norman, K. A., and Kahana, M. J. (2009). A context maintenance and retrieval model
802 of organizational processes in free recall. *Psychological Review*, 116(1):129–156.
- 803 Postman, L. and Phillips, L. W. (1965). Short-term temporal changes in free recall. *Quarterly Journal
804 of Experimental Psychology*, 17:132–138.
- 805 Rabiner, L. (1989). A tutorial on Hidden Markov Models and selected applications in speech
806 recognition. *Proceedings of the IEEE*, 77(2):257–286.
- 807 Radvansky, G. A. and Zacks, J. M. (2017). Event boundaries in memory and cognition. *Curr Opin
808 Behav Sci*, 17:133–140.

- 809 Ramdas, A., Trillos, N., and Cuturi, M. (2017). On wasserstein two-sample testing and related
810 families of nonparametric tests. *Entropy*, 19(2):47.
- 811 Ranganath, C., Cohen, M. X., Dam, C., and D'Esposito, M. (2004). Inferior temporal, prefrontal,
812 and hippocampal contributions to visual working memory maintenance and associative memory
813 retrieval. *Journal of Neuroscience*, 24(16):3917–3925.
- 814 Ranganath, C. and Ritchey, M. (2012). Two cortical systems for memory-guided behavior. *Nature
Reviews Neuroscience*, 13:713 – 726.
- 816 Schlichting, M. L. and Preston, A. R. (2015). Memory integration: neural mechanisms and impli-
817 cations for behavior. *Current Opinion in Behavioral Sciences*, 1:1–8.
- 818 Simony, E., Honey, C. J., Chen, J., and Hasson, U. (2016). Uncovering stimulus-locked network
819 dynamics during narrative comprehension. *Nature Communications*, 7(12141):1–13.
- 820 Spalding, K. N., Schlichting, M. L., Zeithamova, D., Preston, A. R., Tranel, D., Duff, M. C., and
821 Warren, D. E. (2018). Ventromedial prefrontal cortex is necessary for normal associative inference
822 and memory integration. *The Journal of Neuroscience*, 38(15):3767–3775.
- 823 Stark, S. M., Yassa, M. A., and Stark, C. E. L. (2010). Individual differences in spatial pattern
824 separation performance associated with healthy aging in humans. *Learning & Memory*, 17(6):284–
825 288.
- 826 Steyvers, M., Shiffrin, R. M., and Nelson, D. L. (2004). Word association spaces for predicting
827 semantic similarity effects in episodic memory. In Healy, A. F., editor, *Cognitive Psychology and
828 its Applications: Festschrift in Honor of Lyle Bourne, Walter Kintsch, and Thomas Landauer*. American
829 Psychological Association, Washington, DC.
- 830 Tompry, A. and Davachi, L. (2017). Consolidation promotes the emergence of representational
831 overlap in the hippocampus and medial prefrontal cortex. *Neuron*, 96(1):228–241.
- 832 Tyng, C. M., Amin, H. U., Saad, M. N. M., and S, M. A. (2017). The influences of emotion on
833 learning and memory. *Frontiers in psychology*, 8:1454.

- 834 van Kesteren, M. T. R., Beul, S. F., Takashima, A., Henson, R. N., Ruiter, D. J., and Fernández, G.
835 (2013). Differential roles for medial prefrontal and medial temporal cortices in schema-dependent
836 encoding: from congruent to incongruent. *Neuropsychologia*, 51(12):2352–2359.
- 837 van Kesteren, M. T. R., Ruiter, D. J., Fernández, G., and Henson, R. N. (2012). How schema and
838 novelty augment memory formation. *Trends Neurosci*, 35(4):211–9.
- 839 Waskom, M., Botvinnik, O., Okane, D., Hobson, P., David, Halchenko, Y., Lukauskas, S., Cole, J. B.,
840 Warmenhoven, J., de Ruiter, J., Hoyer, S., Vanderplas, J., Villalba, S., Kunter, G., Quintero, E.,
841 Martin, M., Miles, A., Meyer, K., Augspurger, T., Yarkoni, T., Bachant, P., Williams, M., Evans,
842 C., Fitzgerald, C., Brian, Wehner, D., Hitz, G., Ziegler, E., Qalieh, A., and Lee, A. (2016). Seaborn:
843 v0.7.1.
- 844 Welch, G. B. and Burnett, C. T. (1924). Is primacy a factor in association-formation. *American Journal
845 of Psychology*, 35:396–401.
- 846 Wiltgen, B. J. and Silva, A. J. (2007). Memory for context becomes less specific with time. *Learning
847 & Memory*, 14(4):313–317.
- 848 Yassa, M. A., Lacy, J. W., Stark, S. M., Albert, M. S., Gallagher, M., and Stark, C. E. L. (2011). Pattern
849 separation deficits associated with increased hippocampal ca3 and dentate gyrus activity in
850 nondemented older adults. *Hippocampus*, 21(9):968–979.
- 851 Yassa, M. A. and Stark, C. E. L. (2011). Pattern separation in the hippocampus. *Trends In Neuro-
852 sciences*, 34(10):515–525.
- 853 Yonelinas, A. P. (2002). The nature of recollection and familiarity: A review of 30 years of research.
854 *Journal of Memory and Language*, 46:441–517.
- 855 Zacks, J. M., Speer, N. K., Swallow, K. M., Braver, T. S., and Reynolds, J. R. (2007). Event perception:
856 a mind-brain perspective. *Psychological Bulletin*, 133:273–293.
- 857 Zadbood, A., Chen, J., Leong, Y. C., Norman, K. A., and Hasson, U. (2017). How we transmit

858 memories to other brains: Constructing shared neural representations via communication. *Cereb*
859 *Cortex*, 27(10):4988–5000.

860 Zwaan, R. A. and Radvansky, G. A. (1998). Situation models in language comprehension and
861 memory. *Psychological Bulletin*, 123(2):162 – 185.

862 **Supporting information**

863 Supporting information is available in the online version of the paper.

864 **Acknowledgements**

865 We thank Luke Chang, Janice Chen, Chris Honey, Lucy Owen, Emily Whitaker, and Kirsten Ziman
866 for feedback and scientific discussions. We also thank Janice Chen, Yuan Chang Leong, Kenneth
867 Norman, and Uri Hasson for sharing the data used in our study. Our work was supported in part
868 by NSF EPSCoR Award Number 1632738. The content is solely the responsibility of the authors
869 and does not necessarily represent the official views of our supporting organizations.

870 **Author contributions**

871 Conceptualization: A.C.H. and J.R.M.; Methodology: A.C.H., P.C.F. and J.R.M.; Software: A.C.H.,
872 P.C.F. and J.R.M.; Analysis: A.C.H., P.C.F. and J.R.M.; Writing, Reviewing, and Editing: A.C.H.,
873 P.C.F. and J.R.M.; Supervision: J.R.M.

874 **Author information**

875 The authors declare no competing financial interests. Correspondence and requests for materials
876 should be addressed to J.R.M. (jeremy.r.manning@dartmouth.edu).